2018 IEEE International Conference on Robotics and Automation (ICRA)
May 21-25, 2018, Brisbane, Australia

Modeling and Control of Brachiating Robots Traversing Flexible Cables

Siavash Farzan[1], Ai-Ping Hu[2], Evan Davies[3], and Jonathan Rogers[3]

***Abstract*— This paper describes the dynamic modeling and locomotion control of a two-link underactuated brachiating robot traversing a flexible cable. A multi-body system comprised of a two-link robot, a flexible cable, and coupling soft junctions is modeled dynamically. This model is used to formulate an energy-minimizing optimal control strategy that includes the effects of cable vibration induced by robot locomotion. Optimized trajectories and control torque profiles are obtained via multiple-shooting and parametric trajectory approaches. Simulation results show that these optimal torque profiles result in energy-efficient continuous brachiation over a flexible cable. Additional studies examine how the optimal torque profiles change depending on the robot's initial position along a catenary cable.**

I. INTRODUCTION

The past several decades has seen increasing interest in the use of brachiation as a locomotion modality for mobile robots. Brachiation is a form of swinging used efficiently by apes and other mammals to locomote within unstructured environments which contain networks of elevated support structures, such as tree canopies. One attractive aspect of brachiation, compared to other locomotion techniques such as legged locomotion, is that rather than avoiding obstacles, brachiating robots attempt to leverage obstacles as support structures to enable mobility. In fact, brachiation can be viewed as a generalized version of walking in which the contacts with the ground surface or obstacles are adhesive, i.e., the feet of a walking robot become grippers. This generalization allows brachiating robots to be deployed to a wide range of environments, as long as this adhesion or gripping capability can be effectively implemented. The magnetic foot brachiating robot reported by Mazumdar and Asada [1], which is designed to walk inverted below steel bridges, exemplifies this notion of brachiating robots as generalized walking robots.

The authors have prototyped a two-link, single-actuator brachiating robot (affectionately nicknamed "Tarzan") for use with flexible cables, which represents a departure from the literature in which robot brachiation has been reported almost exclusively for relatively rigid rods/supports. The first targeted application for the robot is for performing high throughput phenotyping in a research soybean field that has been arrayed with flexible cables supported by pairs of poles (Fig. 1).

Fig. 1. Tarzan hardware prototype.

Prior work on brachiating robots has primarily focused on derivation of optimal control strategies. Much of this work considers two-link robots, often with a single actuator located between the two links. Similar to gait generation in legged robots, brachiation is often accomplished by specifying a desired link trajectory, and then tracking the link trajectory through the use of a feedback controller. Thus most control schemes employ a feedforward-feedback structure in which the feed-forward portion is driven by the desired link trajectory. The vast majority of prior work has therefore focused on derivation of suitable brachiation trajectories.

Control schemes developed in prior work can be roughly divided into four categories. The first uses heuristics or machine learning to derive link trajectories. Examples include some of the earliest work on brachiation by Fukuda et al. [2], Saito and Fukuda [3] and Hasegawa et al. [4]. Another class of brachiation control laws employs partial feedback linearization ([5], [6]). Model predictive control has also been explored in the context of brachiation, both in a nonlinear [7] and linearized form [8]. Finally, several authors have employed some type of optimal control approach to derive energy-minimizing brachiation gaits (see [9], [10], [11]). Fukuda et al. [12] report experimental results which achieved 30% energy expenditure reduction compared to prior bio-inspired methods. Likewise, Meghdari et al. [10] recently employed an indirect optimal control strategy to derive energy-minimizing swing trajectories, showing a 25% energy reduction compared to the target dynamics method proposed in [13]. Finally, an interesting mechanical design has recently been proposed by Morozovsky and Bewley [14] to address the "rope" (support element parallel to motion

[1]Siavash Farzan is with the School of Electrical and Computer Engineering, Georgia Institute of Technology, Atlanta, GA 30332, USA, sfarzan@gatech.edu

[2]Ai-Ping Hu is with the Georgia Tech Research Institute, Atlanta, GA 30332, USA, ai-ping.hu@gtri.gatech.edu

[3]Evan Davies and Jonathan Rogers are with the Woodruff School of Mechanical Engineering, Georgia Institute of Technology, Atlanta, GA 30332, USA, edavies@gatech.edu and jonathan.rogers@me.gatech.edu

direction) brachiation problem. This system uses clamps to enable a variety of different locomotion modalities along a flexible wire, including an "inchworm" and underhanded swing motions.

While an extensive body of brachiation control research has been established, a key missing element in prior work is treatment of a flexible support in the context of optimal control. To the authors' knowledge, all prior work on optimal brachiation control has assumed a rigid support. In practice, however, brachiating robots will likely need to traverse flexible cables or wires. The main contributions of this paper lie in the formulation of a multi-body dynamic model for a brachiating robot attached to a flexible cable and in the computation of optimal torque trajectories for this configuration. Results are compared to the rigid support case, and the effect of robot placement along a catenary cable on the optimal torque trajectory is quantified. The proposed multi-body model and trajectory optimization approaches may be highly useful in real world applications in which brachiating robots must traverse elevated wires, tree limbs, or other non-rigid support structures.

II. MULTI-BODY DYNAMIC MODEL

This section details the formulation of a multi-body dynamic model comprised of a two-link brachiating robot, lumped-mass flexible cable, and soft junction that connects the robot to the cable. The advantage of using this type of multi-body formulation is that the dynamic interaction between the robot and the cable is captured, and control laws and the physical system can be designed to avoid unwanted vibrational modes. Likewise, control laws and physical parameters can also be designed to recapture cable vibrational energy to reduce the energy expended by the robot during swinging maneuvers. It is important to note that the model considered here is planar; off-axis or lateral motion of the robot and cable is not considered. Each element of the multi-body model is detailed in the following subsections.

A. Two-Link Brachiating Robot

The two-link brachiating robot is modeled as a rigid body in planar motion consisting of two rotational and two translational degrees of freedom (DOF): θ_1 and θ_2 are the angles of the first and the second links with respect to the vertical axis and $x_{g,1}$ and $z_{g,1}$ denote the Cartesian position of the robot's gripper that is attached to the cable (i.e., via the soft junction to be discussed below). The configuration of the robot, from which the system dynamics are obtained, is shown in Fig. 2. The system is underactuated, with the robot's single torque actuator located at the joint between the two links. The actuator is considered massless, and any payload mass is distributed between and lumped with the mass of the two links (m_{L1} and m_{L2}). The dynamic model for such a system, which is known as a compound double pendulum, is given by eight differential equations of motion. These equations are omitted here for space considerations but are available in [6]. It is important to note, however, a key difference between the model employed here and a standard double pendulum available in the physics literature. In the model used here, the position of the gripper is not considered fixed in inertial space, and thus its position $(x_{g,1}, z_{g,1})$ and velocity $(\dot{x}_{g,1}, \dot{z}_{g,1})$ must be considered as state variables in addition to the two link angles.

Soft junction forces $\vec{F}_{SJ,1}$ and $\vec{F}_{SJ,2}$ act on each gripper (at the ends of each link) if the gripper is attached to the cable. These forces act in addition to gravity and are only active when a gripper is attached. Thus, the standard compound double pendulum equations of motion are modified to include the translational accelerations and torques generated by the soft junction forces as Eq. (1), where $\vec{x}_R$ represents the state vector of the robot, and u is the torque applied by the actuator.

$$\ddot{\vec{x}}_R = \vec{f}(\vec{x}_R, \dot{\vec{x}}_R, \vec{F}_g, \vec{F}_{SJ,1}, \vec{F}_{SJ,2}, \vec{u}) \tag{1}$$

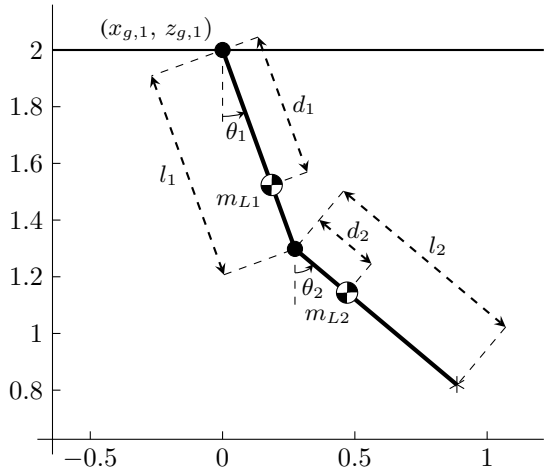

Fig. 2. The model of the two-link brachiating robot used in this paper.

B. Flexible Cable

Several methods for modeling flexible cables have been presented in the literature for a variety of applications. Some examples of flexible cable modeling techniques can be found in [15], [16], [17], [18], [19], [20], and [21]. Among these methods, the finite-element approach ([22], [23]) is one of the most versatile. In this method the cable is represented as an arbitrary number of segments joined at nodes. The segments are modeled in different ways: massless straight lines or springs, straight rigid cylinders, or curved rigid segments. The equations of motion are derived for each segment and the description of the behavior of the entire cable is obtained by solving a system of ODEs.

In the present work, a variation of the finite-element or lumped-mass method is used to model the flexible cable. A continuous cable with length l_c is represented as a series of $n-1$ point-mass elements joined by n connection segments (where the walls at the end points of the cable are considered fixed positions). Each connection segment is modeled as a parallel linear spring and damper, with unstretched length of $l_s = l_c/n$ (Fig. 3). To derive the equations governing the motion of the cable elements, each element requires two new generalized coordinates (x_i and z_i) which are the inertial

positions of lumped-mass element i. The equations of motion for the lumped-mass system can be derived by considering lumped-mass element i. The total forces exerted on element i resolved into the inertial x and z directions are given by:

$$\begin{aligned}\vec{F}_{x,i} = & k_c(\frac{l_{i+1}-l_s}{l_{i+1}})(x_{i+1}-x_i) \\ & - k_c(\frac{l_i-l_s}{l_i})(x_i-x_{i-1}) \\ & + b_c(\dot{x}_{i+1}-\dot{x}_i) - b_c(\dot{x}_i-\dot{x}_{i-1}) \\ & + \vec{F}_{SJ,x,1} + \vec{F}_{SJ,x,2}\end{aligned} \tag{2}$$

and

$$\begin{aligned}\vec{F}_{z,i} = & k_c(\frac{l_{i+1}-l_s}{l_{i+1}})(z_{i+1}-z_i) \\ & - k_c(\frac{l_i-l_s}{l_i})(z_i-z_{i-1}) \\ & + b_c(\dot{z}_{i+1}-\dot{z}_i) - b_c(\dot{z}_i-\dot{z}_{i-1}) \\ & - mg + \vec{F}_{SJ,z,1} + \vec{F}_{SJ,z,2}\end{aligned} \tag{3}$$

where l_s is the unstretched length of the segment and:

$$l_i = ((x_i - x_{i-1})^2 + (z_i - z_{i-1})^2)^{\frac{1}{2}}.$$

$\vec{F}_{SJ,x,1}$, $\vec{F}_{SJ,x,2}$, $\vec{F}_{SJ,z,1}$, and $\vec{F}_{SJ,z,2}$ are the soft junction forces to be described in the next section. Applying Newton's Second Law to each element in the x and z directions yields a linear system of $n-1$ ODEs of the form $\dot{X} = AX$, where X is the vector of position and velocity states and A is constructed from the kinematics and total force on each element given in Eqs. (2) and (3). The linear differential equations in Eqs. (2) and (3) can be written for the x and z directions yielding a total of $2(n-1)$ equations. These can be integrated with respect to time to compute the motion of the lumped-mass cable.

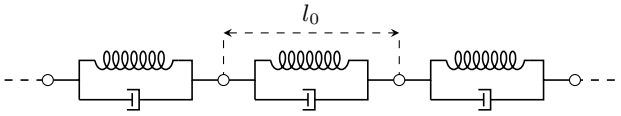

Fig. 3. Dynamic model of the cable using the finite-element method, shown in unstretched position.

C. Soft Junctions

The coupling dynamics between the robot and the flexible cable is modeled as a soft junction. In this approach, it is assumed that the robot is attached to the cable via a stiff spring-damper. The model provides the ability to capture relative vibrations and collisions taking place between the robot's grippers and the cable. The grippers can be attached anywhere on a connection segment between two nodes. Each node's contribution to the soft junction forces in the equations of motion are calculated based on the position of the attachment, as depicted in Fig. 4. A normalized ratio r and $1-r$ is applied to the position and velocity of the bracketing nodes, used to compute spring potential energy and the damping dissipation, respectively. The position of the soft junction is the same as the two translational coordinates of the attached gripper (i.e., link endpoint).

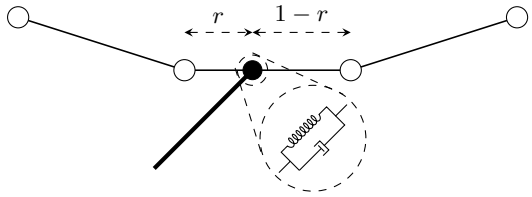

Fig. 4. A soft junction between the robot's gripper and a segment of the flexible cable.

For a soft junction with position $x_{g,j}$ attached to the segment i (between nodes i and $i+1$) with ratios of r and $1-r$, the soft junction force is calculated as:

$$\begin{aligned}\vec{F}_{SJ,j,x} = & k_{SJ}(x_{g,j} - (rx_i + (1-r)x_{i+1})) \\ & + b_{SJ}(\dot{x}_{g,j} - (r\dot{x}_n + (1-r)\dot{x}_{n+1}))\end{aligned} \tag{4}$$

for $j \in 1, 2$, with analogous expressions for the z direction. In Eq. (4), k_{SJ} and b_{SJ} are the soft junction stiffness and damping coefficients, respectively. Note that these coefficients do not, in general, have the same values as the stiffness and damping used in the cable connection segments.

By combining the above dynamical models described in sections II-A, II-B and II-C, the multi-body dynamic model has a total of $4 + 2(n-1)$ generalized coordinates: two rotational DOFs (θ_1, θ_2) of the robot, two translational coordinates of the one of the grippers, and $2(n-1)$ translational coordinates for the nodes of a cable discretized into $n-1$ lumped mass elements. Given the state vectors of the robot and cable respectively as, $\vec{x}_R = [\theta_1, \theta_2, x_{g,1}, z_{g,1}]^T$ and $\vec{x}_C = [x_1, z_1, ..., x_{n-1}, z_{n-1}]^T$, the state vector of the combined system is given by $\vec{x} = [\vec{x}_R^T, \vec{x}_C^T]^T$.

D. Collision Detection via Instantaneous Switch

When modeling the robot performing multiple sequential swinging maneuvers, the soft junction mechanism between the robot and cable must be activated and deactivated. There are a variety of methods for modeling contact forces and for activating soft contact models when bodies collide [24]. In this paper, an instantaneous switching method is employed to model between release from and engagement with the cable.

Consider the case of a free gripper coming into contact with the cable. When gripper j is free, its soft junction parameters $k_{SJ,j} = 0$ and $b_{SJ,j} = 0$. To determine when the soft junction should be activated, the exact time of collision is detected as follows. At each timestep, a geometric analysis is performed to determine whether gripper j has passed from one side of the cable to the other. If it has, a step-halving process is employed to determine the time at which the gripper crosses a certain distance threshold r_t from the closest cable connection segment. Once this time is found, the system state is saved as a new initial condition. The soft junction parameters are then set to $k_{SJ,j} = k_{SJ}$ and $b_{SJ,j} = b_{SJ}$ (their nominal values during activation) and integration of the system equations of motion resume from this new initial condition. For all example cases shown below, a threshold distance of $r_t = 1$ mm is used.

III. OPTIMAL MOTION CONTROL

The primary goal of the optimal control studies performed here is to minimize energy consumption of the brachiating robot attached to the flexible cable over one single, underhanded brachiating swing. This has practical benefits by enabling the use of smaller batteries, motors, and power supplies, or equivalently enabling longer operation between recharging cycles (or even the ability to create a solar-powered system). Two methods are employed in this work to generate optimal trajectories. The first technique combines a multiple shooting method [25] with nonlinear programming [26] to solve for a minimal torque trajectory using zero velocity boundary condition constraints. These zero velocity constraints are imposed in order to minimize energy dissipation at the collision between robot gripper and cable [9]. While this technique yields highly general trajectory shapes, it becomes impractical when applied to the flexible cable described in the previous section due to the large size of the state space and the stiff nature of the multi-body system. A second approach is therefore employed in the form of a parametric trajectory optimization. In this technique, the optimal torque input is represented as an n-degree polynomial or n-harmonic Fourier series, and the optimal polynomial parameters or Fourier coefficients are derived through a gradient-based parameter optimization process. This parametric trajectory optimization approach can be applied much more effectively in the flexible cable problem due to its lower computational complexity in comparison with the multiple shooting method. In this second method the zero-velocity terminal constraint on the free gripper is imposed as well.

The optimization cost function for the cases studied here seeks design a trajectory that minimizes a quadratic cost function of $u^2(t)$ while satisfying a set of constraints including the dynamics (equations of motion), initial and final positions (determined by cable geometry), and zero velocity boundary conditions. This leads to a constrained optimization problem that can be stated in general form as:

$$\begin{aligned} \text{minimize:} \quad & f(x) \\ \text{with respect to:} \quad & x \in S \\ \text{subject to:} \quad & h_i(x) = 0,\ i = 1, 2, ..., m \\ & g_j(x) \leq 0,\ j = 1, 2, ..., r \end{aligned}$$

where x is an n-dimensional vector of unknowns, S is a subset of n-dimensional space. The function f is the objective function of the problem, while $h(x)$ and $g(x)$ represent the equality and inequality constraints, respectively. This form will be used in the following sections to define the trajectory optimization problem.

A. Multiple Shooting

The multiple shooting method for the torque optimization problem is formulated as follows. A final time t_f is selected and the time interval $[t_0, t_f]$ is divided into n_s equally-spaced intervals, as shown in Fig. 5. Each interval has its own unknown initial state x_0^k and unknown control function u_k. For grid k, the differential equations of motion are integrated from t_k to the end of the grid at t_{k+1}, with the final state denoted by x_f^k. During this integration a constant input torque u_k is applied, with $u_k \neq u_{k+1}$ in general. The total cost is minimized subject to the system's dynamics and constraints to ensure that the state is continuous across all grids, i.e., the defect/discontinuity $d_k := x_0^{k+1} - x_f^k = 0$ $\forall k$ to ensure that the grids join at the boundaries as shown in Fig. 5). The parameters that are optimized in this case are the set of constant control inputs u_k, $k = 1, ..., n$ such that $|u_k| \leq u_{max}$. For all cases shown here, a value of $u_{max} = 5$ Nm is selected.

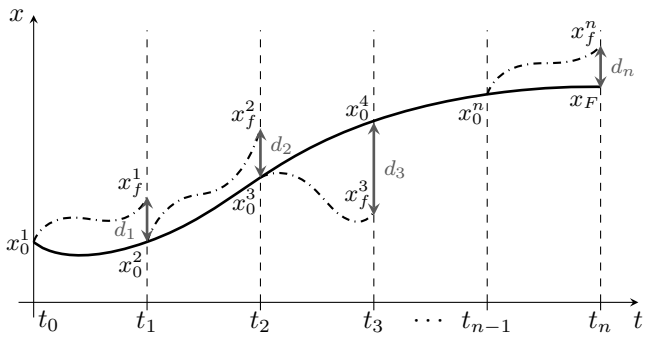

Fig. 5. Multiple shooting grids and the discontinuity at boundaries.

The built-in MATLAB gradient-based optimization routine "fmincon" is used to solve the nonlinear programming problem. The torque optimization problem is formally stated as follows:

$$\begin{aligned} \underset{u_k}{\text{minimize:}} \quad & J(u) = \sum_{k=1}^{n} u_k^2 \\ \text{subject to:} \quad & q_0 = \text{initial conditions} \\ & \theta_1(t_f) = \tfrac{\pi}{4},\ \theta_2(t_f) = \tfrac{3\pi}{4} \\ & \dot{\theta}_1(t_f) = 0,\ \dot{\theta}_2(t_f) = 0 \\ & d_k = 0\ \forall k \\ & |u(t)| \leq 5 \end{aligned}$$

where q is the general coordinates of the robot, u is the torque applied by the actuator, and d_k are the defects between consecutive grids. As shown in Eq. (III-A), the defects and initial and final states are all defined as equality constraints, although in practice they are minimized to some small tolerance. An initial guess for the states at each interval boundary x_0^k and the control inputs u_k over each interval is provided to the algorithm. Note that there is a trade-off between using a large number of grids (thereby achieving a better solution) and computation time. This balance will be discussed further in Section IV.

B. Parametric Trajectory Model

By including the flexible cable dynamics in the brachiating robot system, the equations of motion of the problem become a stiff set of ODEs [27], meaning that the step size is dictated by stability requirements rather than by accuracy concerns. In that case, the system needs to be forward integrated with an extremely small step size. The multiple shooting method described in III-A is difficult to implement for this problem

due to the large number of intervals that are required for convergence to a solution. Instead, by characterizing the final torque trajectory to lie within a family of parametric curves, the constrained optimization process is reduced from finding the control values (u) at each interval to calculating the coefficients of a parametric curve, such as a polynomial or Fourier series. This dimensionality reduction is beneficial both in terms of convergence properties and computation time.

1) Polynomials: The torque trajectory is represented by an n-degree polynomial, $p(t)$,

$$p(t) = p_1 t^n + p_2 t^{n-1} + \cdots + p_n t + p_{n+1} \tag{5}$$

The objective of the optimization problem is to calculate the $n+1$ polynomial coefficients, p_i, while satisfying the functional constraints and boundary conditions. Using higher-order polynomials allows the trajectory to take on a more generalized shape, meaning that the curve can better represent the optimal solution. However, due to the rigidity and smoothness of polynomials, there is a risk of incurring Runge's phenomenon [28] and over-fitting data. Moreover, higher-order polynomials require the NLP solver to estimate more coefficients, increasing the risk of converging to local minima or even not converging. Therefore, the optimum polynomial degree must be explored through some degree of trial and error.

2) Fourier Series: When using this parameterization, the torque trajectory is represented as a Fourier series with n harmonics and the fundamental frequency f_0. The goal of the optimization problem is to estimate the $2n+1$ coefficients (a_i and b_i) of the Fourier series:

$$f(t) = a_0 + \sum_{i=1}^{n} \left(a_i \cos(i2\pi f_0 t) + b_i \sin(i2\pi f_0 t)\right) \tag{6}$$

While Fourier series are better able to represent periodic trajectories compared to polynomials, a poor choice of the initial fundamental frequency can lead to a poor solution or even lack of convergence. Therefore, in practice the trajectory may be optimized for various fundamental frequencies and their resulting cost compared, or the f_0 may be included as an additional parameter in the optimization.

To implement this method, an initial guess for total time (t_f) and coefficients (p_i for polynomials or a_i, b_i for Fourier series) is provided to the NLP solver. The fundamental frequency f_0 of the Fourier series could be another parameter optimized by the algorithm, or a fixed guess could be used. The equality constraints are defined as the initial/final positions and zero boundary velocities of the robot. This constrained optimization problem can be stated as:

$$\begin{aligned}
\underset{p_i \text{ or } (a_i,b_i,f)}{\text{minimize:}} \quad & J(u) = \int_{t_0}^{t_f} u^2 dt \\
\text{subject to:} \quad & q_I = \text{initial conditions} \\
& \dot{\theta}_1(t_f) = 0,\ \dot{\theta}_2(t_f) = 0 \\
& |u(t)| \leq 5 \\
& 1 \leq (x_{g,2}(t_f) - x_{g,1}(t_f)) \leq 1.025 \\
& |z_{g,2}(t_f) - z_c(t_f)| \leq 0.001
\end{aligned}$$

where q are the generalized coordinates of the robot, $(x_{g,2}, z_{g,2})$ represents the position of the free gripper of the robot, (x_c, z_c) represents the position of the closest point on the cable to the free gripper, and $x_{g,1}$ the horizontal element of the soft junction of the pivot gripper attached to the cable.

For both the polynomial and Fourier series trajectory optimization schemes, the MATLAB gradient-based solver fmincon is used to compute the trajectory solution. The results of the several example cases will be described in the next section.

IV. RESULTS AND DISCUSSION

The simulation of the dynamic model as well as the optimal torque trajectory calculations are performed in the MATLAB software environment. The proposed algorithm is applied to two problems: brachiation along a rigid bar, and along a flexible cable. The solutions are compared and differences due to cable flexibility are noted. The physical parameters of the flexible cable and soft junctions used in the simulation experiments are shown in Table I. The length of each arm of the robot is 0.71 m and the total weight of the robot is 4 kg. The arms are modeled as rods with negligible thickness, and so the moments of inertia are given by $\frac{1}{12}ml^2$. The center of mass of each link is located at one-third the distance from the central link connection, since the weight of the actuator and the payload comprise about two-thirds of the total robot weight. For the simulations with a flexible cable, an 8 m cable is used. The segments for the finite element method are chosen with an interval length of 20 cm, resulting in 40 segments and 39 free nodes in total. The dynamics of the system are modeled as described in Section II, resulting in 82 second-order differential equations of motion, which are represented as 164 first-order ODEs and integrated over time using the RK4 method. In the case of brachiation over the flexible cable, the step size is set to a sufficiently small value (0.1 ms) for the Runge-Kutta method to avoid instability, while in the case of rigid bars the integration can use much larger step sizes (i.e., 50 ms).

TABLE I
PHYSICAL PARAMETERS OF THE SIMULATED FLEXIBLE CABLE AND SOFT JUNCTIONS

Parameter		*Value*
Cable length	l_c	8 m
Cable linear mass	m_c	0.5 kg/m
Cable stiffness	k_c	785400 N/m
Cable damping	b_c	4
Soft junction stiffness	k_{SJ}	8000 N/m
Soft junction damping	b_{SJ}	5

A. Optimal Control via Multiple Shooting over Rigid Bar

The optimized torque profile for brachiation along a rigid bar is computed using the multiple shooting method. The number of grids for the multiple shooting is set to 20, as using more grids was found to result in almost the same trajectory and achieved cost. The robot starts from rest with $\theta_1 = -45^\circ$ and $\theta_2 = -135^\circ$. The final desired state is $\theta_1 = 45^\circ$ and $\theta_2 = 135^\circ$ (which is the symmetric posture of the

initial configuration about the z axis) with zero velocity, to ensure a plastic collision. Torque is limited to values within ± 5 Nm.

The determined optimal trajectory for "underhand" brachiation is shown in Fig. 6. The total cost is 2.33 $\mathrm{N^2m^2}$, and the resultant open-loop joint torque is within ± 2.5 N m, well within the torque capabilities of a fairly low-cost off-the-shelf motor. The duration of the optimized brachiation trajectory is about 1.1 seconds from cable release to cable re-engagement, which results in a linear payload motion of about 1 meter.

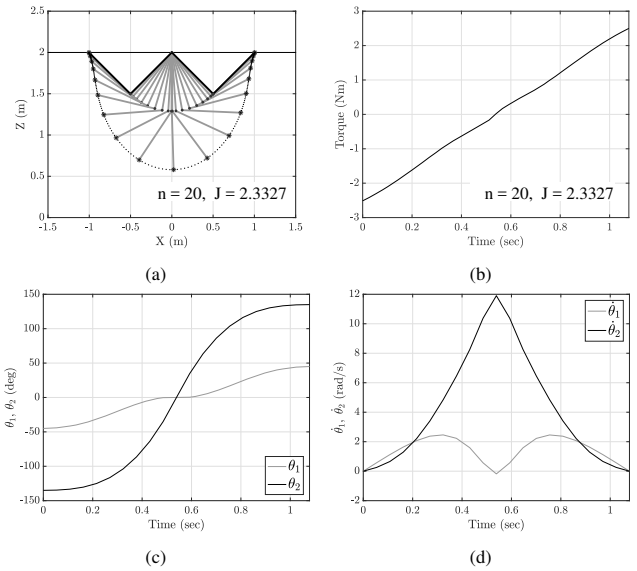

Fig. 6. Underhand brachiation on rigid bar (a) Robot motion trajectory (b) Optimal torque profile (c) Joint trajectories (d) Joint velocities

It is interesting to consider a case in which the final velocity constraint is lifted, meaning that the robot gripper can collide with the cable at a nonzero speed. While this may have negative practical consequences in terms of probability of capturing the cable (due to collision and rebound), the optimal torque trajectory for this case was computed resulting in a reduced final cost from 2.33 $\mathrm{N^2m^2}$ (with the constraint) to 1.03 $\mathrm{N^2m^2}$ (without it). Thus, if some final velocity can be tolerated by the gripper, the potential for energy expenditure reduction is significant.

B. Optimal Control via Parametric Trajectory over a Flexible Cable

The parametric trajectory method using a polynomial is applied to the underhand brachiation problem on a flexible cable. To find the initial conditions of the robot and the cable, the robot with configuration of $\theta = [-45°, -135°]$ is attached to a straight cable and the system is simulated forward in time for a long enough duration such that the system reaches steady-state. This so-called "trimming " process is oftentimes used in multi-body dynamics modeling to establish a steady-state initial condition from which motion can be simulated. As stated in Section III-B, the desired final configuration of the robot is to reach within a 1 millimeter vertical tolerance from the cable ($|z_{g,2}(t_f) - z_c(t_f)| \leq$

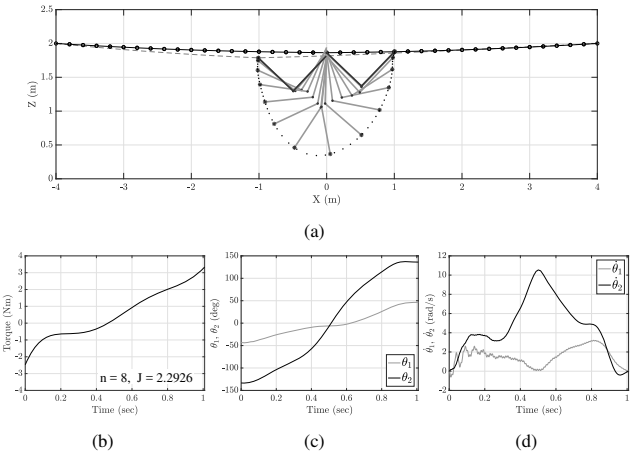

Fig. 7. Underhand brachiation over flexible cable using polynomial parametric trajectory, starting from center (a) Robot motion trajectory (b) Optimal torque profile (c) Joint trajectories (d) Joint velocities

0.001), while the swinging gripper is located horizontally 1 meter away from the pivot gripper with a 25 millimeter tolerance ($1 \leq (x_{g,2}(t_f) - x_{g,1}(t_f)) \leq 1.025$). This maintains the swing-to-swing symmetric position of the robot while ensuring that it traverses the desired length of the cable.

The resulting states and optimal torque trajectory using a polynomial of degree 8 are presented in Figs. 7-9. Note that the steady-state condition of the cable is a catenary geometry, and thus the optimal torque profile will be different depending on whether the robot starts at the left (swinging left to right "downhill"), center (swinging level), or right (swinging "uphill"). These cases are shown respectively in Figs. 7-9. The duration of the optimized brachiation trajectory is about 1 second and the total cost is between 2.3 $\mathrm{N^2m^2}$ to 3.9 $\mathrm{N^2m^2}$ depending on the position of the robot. The resultant joint torque is within ± 5 N m. Note that the same general trend in the torque trajectory is observed between the flexible cable torque profiles and those of the bar, but some asymmetries in the flexible cable profiles are clearly observed. This is due to the cable vibration that is induced as the swing progresses, which results in a torque profile that is different during the second half of the maneuver compared to the first. It was observed that the resulting optimization cost continued to decrease when using higher-degree polynomials, until about degree 8 after which the cost reductions were minimal. Also note that the initial state of the system, specifically for the cable, can significantly affect the resultant torque trajectory, as will be discussed further in Section IV-C.

To improve confidence that the trajectory shown in Fig. 7 is in fact close to the optimal solution, the Fourier trajectory parameterization is also used to calculate the optimal torque trajectory for underhand brachiation. The resultant states and optimized torque trajectory using a Fourier series with 8 harmonics are illustrated in Fig. 10. In this case the optimizer converged to a fundamental frequency of $f_0 = 0.15242$. The results in Fig. 10 are nearly identical to the corresponding case using polynomials, suggesting that this is indeed close to the global optimal solution and not a local minimum. Note that using more harmonics greater than 6 improved the cost

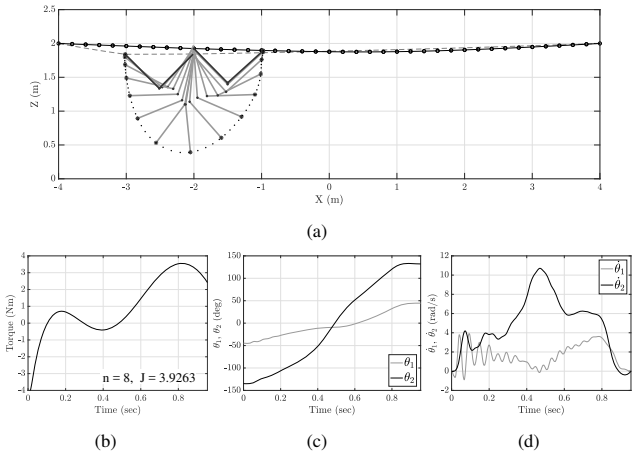

Fig. 8. Underhand brachiation over flexible cable using polynomial parametric trajectory, starting from left (a) Robot motion trajectory (b) Optimal torque profile (c) Joint trajectories (d) Joint velocities

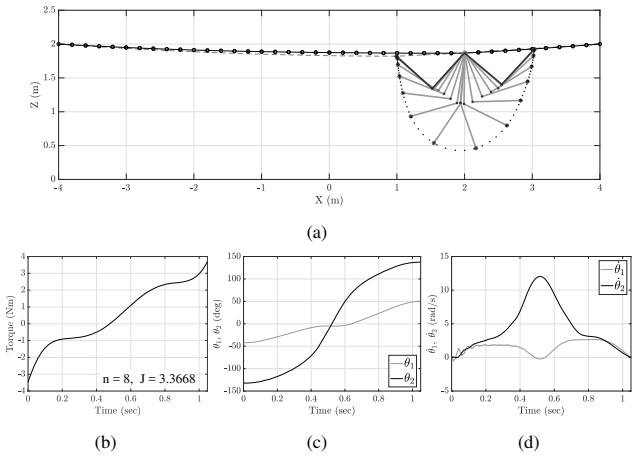

Fig. 9. Underhand brachiation over flexible cable using polynomial parametric trajectory, starting from right (a) Robot motion trajectory (b) Optimal torque profile (c) Joint trajectories (d) Joint velocities

function only slightly, and had the primary effect of lowering the computed optimal fundamental frequency. Overall, the torque profile remained mostly unchanged using more than 6 harmonics.

A summary of the results for brachiation over flexible cable including the cost and brachiation time is presented in Table II.

TABLE II

FINAL COST AND DURATION FOR BRACHIATION OVER FLEXIBLE CABLE

Method / Starting point	*Cost* (N^2m^2)	*Brachiation Time (sec)*
Polynomial / Left	3.9263	0.9548
Polynomial / Center	2.2926	1.0083
Polynomial / Right	3.3668	1.0482
Fourier / Center	2.4165	0.9962

C. Continuous Brachiation over Flexible Cable

It is interesting to examine how the optimal torque profiles change when the robot performs multiple, sequential swings ("continuous" brachiation). This results in the robot beginning from non-zero dynamic states for all except the first swing, as the rope continues to vibrate. Continuous

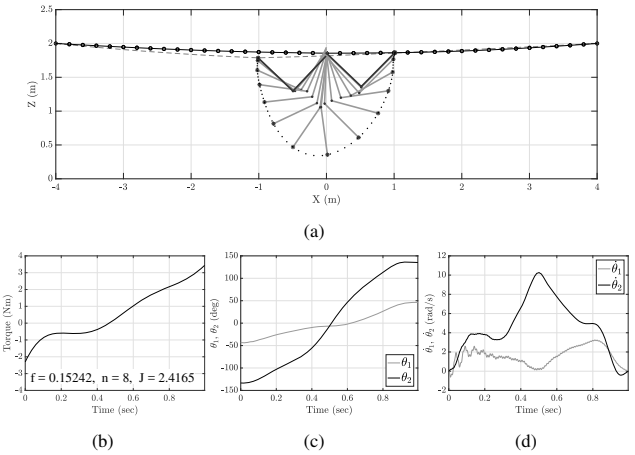

Fig. 10. Underhand brachiation over flexible cable using Fourier series parametric trajectory, starting from center (a) Robot motion trajectory (b) Optimal torque profile (c) Joint trajectories (d) Joint velocities

brachiation is performed on an 8 meter flexible cable (discretized into 40 segments and 39 nodes) by employing the polynomial parametric trajectory method with degree 8. The robot traverses almost the entire length of the cable in 5 swings. The resulting motion trajectory and optimized torque are shown in Fig. 11. Note that there is a pause of between 1 to 1.2 seconds enforced between sequential swings. The final cost varies for different swings from 1.16 $\mathrm{N^2m^2}$ to 4.54 $\mathrm{N^2m^2}$, depending on the swing number. Comparing these values against those for steady-state brachiation in Table II, it is clear that the energy expenditure may be lower or higher depending on the phase of the cable vibration at the attached gripper. For instance, in swing 3, the energy expended was significantly lower since the robot was able to take advantage of the cable vibration to assist its swing trajectory. Conversely, the cost for swing 4 was higher than in the static case because the robot had to overcome counteract motion in the wrong direction to complete the swing. This suggests that if the starting point of the swing maneuvers are timed correctly, the effect of the cable can be advantageously used to inject energy from the cable to the robot motion, thereby reducing cost and resulting in more energy-efficient swings than if the cable motion was ignored. Such additional advancements, while shown to be feasible in these results, are beyond the scope of this paper and will be the subject of future work. (Simulation video of this continuous brachiation, as well as results presented in previous sections, can be found in the accompanying video for the paper.)

V. CONCLUSIONS AND FUTURE WORK

The dynamic modeling of a multi-body system consisting of a brachiating robot traveling along a flexible cable has been presented. The system consists of a two-link brachiating robot, the flexible cable it is traversing, and the associated soft junctions for coupling the robot to the cable. A finite-element method has been used to derive the equations of motion for the cable. Numerical simulation results have been presented for continuous brachiation on a rigid bar (as a base-

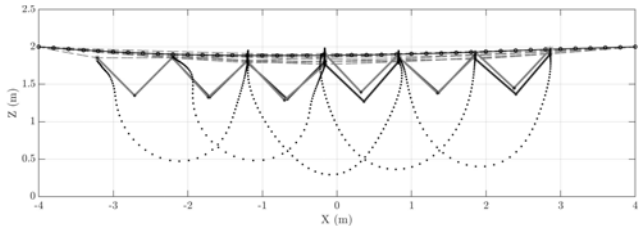

(a)

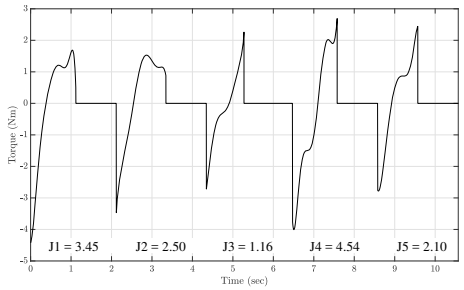

(b)

Fig. 11. Continuous brachiation on a flexible cable via polynomial parametric trajectory (a) Robot motion trajectory (b) Optimal torque profile

line reference) and on a flexible cable. An optimal control scheme has been designed to compute energy-efficient torque trajectories using multiple shooting and parametric trajectory methods. For the latter, both polynomial curves and Fourier series trajectory representations have been explored. The optimal torque profiles for the rigid bar and flexible cable cases showed the same general trends, but cable vibration induced by the robot motion leads to asymmetric torque profiles. In cases where the robot performs multiple sequential swings (or the cable is vibrating at swing initiation), it is shown that the robot may harness the cable vibrational energy to reduce its own energy expenditure.

In this work, the proposed optimal trajectories are applied to the robot as an open-loop feedforward command. Future work will seek to design a closed-loop controller to be used in conjunction with the feedforward strategy, in order to make the system robust to external perturbations. The observed effect of energy being transferred from the cable to the brachiating robot will also be explored further, with the aim of achieving even greater energy efficiency while performing continuous brachiation.

REFERENCES

[1] A. Mazumdar and H. H. Asada, "An underactuated, magnetic-foot robot for steel bridge inspection," *Journal of Mechanisms and Robotics*, vol. 2, no. 3, p. 031007, 2010.

[2] T. Fukuda, H. Hosokai, and Y. Kondo, "Brachiation type of mobile robot," in *Advanced Robotics, 1991. 'Robots in Unstructured Environments', 91 ICAR., Fifth International Conference on*, June 1991, pp. 915–920 vol.2.

[3] F. Saito, T. Fukuda, and F. Arai, "Swing and locomotion control for two-link brachiation robot," in *[1993] Proceedings IEEE International Conference on Robotics and Automation*, May 1993, pp. 719–724 vol.2.

[4] Y. Hasegawa, T. Fukuda, and K. Shimojima, "Self-scaling reinforcement learning for fuzzy logic controller-applications to motion control of two-link brachiation robot," *IEEE Transactions on Industrial Electronics*, vol. 46, no. 6, pp. 1123–1131, Dec 1999.

[5] M. W. Spong, "Partial feedback linearization of underactuated mechanical systems," in *Intelligent Robots and Systems '94. 'Advanced Robotic Systems and the Real World', IROS '94. Proceedings of the IEEE/RSJ/GI International Conference on*, vol. 1, Sep 1994, pp. 314–321 vol.1.

[6] ——, "The swing up control problem for the acrobot," *IEEE Control Systems*, vol. 15, no. 1, pp. 49–55, Feb 1995.

[7] V. M. de Oliveira and W. F. Lages, "Control of a brachiation robot with a single underactuated joint using nonlinear model predictive control," *IFAC Proceedings Volumes*, vol. 40, no. 20, pp. 430 – 435, 2007.

[8] ——, "Mpc applied to motion control of an underactuated brachiation robot," in *2006 IEEE Conference on Emerging Technologies and Factory Automation*, Sep 2006, pp. 985–988.

[9] M. W. Gomes and A. L. Ruina, "A five-link 2d brachiating ape model with life-like zero-energy-cost motions," *Journal of Theoretical Biology*, vol. 237, no. 3, pp. 265 – 278, 2005.

[10] A. Meghdari, S. M. H. Lavasani, M. Norouzi, and M. S. R. Mousavi, "Minimum control effort trajectory planning and tracking of the cedra brachiation robot," *Robotica*, vol. 31, no. 7, pp. 1119–1129, 2013.

[11] H. Kajima, M. Doi, Y. Hasegawa, and T. Fukuda, "Energy based swing control of a brachiating robot," in *Proceedings of the 2005 IEEE International Conference on Robotics and Automation*, April 2005, pp. 3670–3675.

[12] T. Fukuda, S. Kojima, K. Sekiyama, and Y. Hasegawa, "Design method of brachiation controller based on virtual holonomic constraint," in *2007 IEEE/RSJ International Conference on Intelligent Robots and Systems*, Oct 2007, pp. 450–455.

[13] J. Nakanishi, T. Fukuda, and D. E. Koditschek, "A brachiating robot controller," *IEEE Transactions on Robotics and Automation*, vol. 16, no. 2, pp. 109–123, Apr 2000.

[14] N. Morozovsky and T. Bewley, "Skysweeper: A low dof, dynamic high wire robot," in *2013 IEEE/RSJ International Conference on Intelligent Robots and Systems*, Nov 2013, pp. 2339–2344.

[15] Y.-i. Choo and M. J. Casarella, "A survey of analytical methods for dynamic simulation of cable-body systems." *Journal of Hydronautics*, vol. 7, no. 4, pp. 137–144, 1973.

[16] C. A. Hill, "Theoretical modeling of the transient effects of a towline using the method of characteristics," Master's thesis, Air Force Institute of Technology, Wright-Patterson AFB Ohio, Graduate School of Engineering and Management, 2006.

[17] G. F. Giaccu and L. Caracoglia, "Effects of modeling nonlinearity in cross-ties on the dynamics of simplified in-plane cable networks," *Structural Control and Health Monitoring*, vol. 19, no. 3, pp. 348–369, 2012.

[18] ——, "Generalized power-law stiffness model for nonlinear dynamics of in-plane cable networks," *Journal of Sound and Vibration*, vol. 332, no. 8, pp. 1961 – 1981, 2013.

[19] J. Goeller and P. Laura, "Analytical and experimental study of the dynamic response of segmented cable systems," *Journal of Sound and Vibration*, vol. 18, no. 3, pp. 311 – 324, 1971.

[20] P. Williams and P. Trivailo, "Dynamics of circularly-towed aerial cable systems, part 1: Optimal equilibrium configurations and their stability," *Journal of Guidance, Control, and Dynamics*, 2007.

[21] G. Frost and M. Costello, "Improved deployment characteristics of tether-connected munition systems," *Journal of Guidance, Control, and Dynamic*, vol. 24, no. 3, pp. 547–554, 2001.

[22] T. S. Walton and H. Polachek, "Calculation of transient motion of submerged cables," *Mathematics of computation*, vol. 14, no. 69, pp. 27–46, 1960.

[23] B. Buckham and M. Nahon, "Dynamics simulation of low tension tethers," in *OCEANS '99 MTS/IEEE. Riding the Crest into the 21st Century*, vol. 2, 1999, pp. 757–766 vol.2.

[24] P. Flores and H. Lankarani, *Contact Force Models for Multibody Dynamics*, ser. Solid Mechanics and Its Applications. Springer International Publishing, 2016.

[25] J. Betts, *Practical Methods for Optimal Control and Estimation Using Nonlinear Programming*, 2nd ed. Society for Industrial and Applied Mathematics, 2010.

[26] D. Luenberger and Ye, *Linear and Nonlinear Programming*, 3rd ed. Springer, 2008.

[27] W. H. Press, S. A. Teukolsky, W. T. Vetterling, and B. P. Flannery, *Numerical Recipes 3rd Edition: The Art of Scientific Computing*, 3rd ed. New York, NY, USA: Cambridge University Press, 2007.

[28] L. N. Trefethen and J. Weideman, "Two results on polynomial interpolation in equally spaced points," *Journal of Approximation Theory*, vol. 65, no. 3, pp. 247–260, 1991.